The applications of nano-hetero-junction in optical and thermal catalysis

Fenglin Liao,[a] Benedict T.W. Lo,[a] and Edman Tsang*[a]

Abstract: Semi-conductors, particularly metal oxides, are usually regarded as one of the key components in most industrial catalysts. It has been reported that the band structure of semi-conductors can significantly influence their catalytic properties. As one of the most effective methods for tuning the band structure of semi-conductors, the establishment of nano-hetero-junction in catalyst, is getting increasing attentions due to the rational design and the facile synthesis procedure. This mini-review scoops the applications of nano-hetero-junction in both photo- and traditional thermal-catalytic reactions. These reactions range from pollutants removal, renewable energy production to new chemical synthesis routes, all of which are closely knitted to our daily life. In photo-catalysis, the improvement is mainly attributed to the separation of photo-generated electrons and holes, which prolongs their lifetime and eventually allows the occurrence of chemical reactions with the adsorbed substrate molecules. Our research group were amongst the first to apply this concept into designing metal/metal oxide catalysts in traditional thermal-catalysis. It is found the establishment of electronic nano-hetero-junction in support material using two semiconducting metal oxides of different energy levels influences the catalytic properties of the dispersed metal particles from two perspectives: i) the potential energy upon exicitation, created by the charge separation on semi-conducting oxide support in proximity to the overlying metal particles; ii) under H_2 atmosphere, the accumulated electrons on one semiconducting oxide support can facilitate direct reduction of metal cations in this support to metal atoms, while the accumulated holes (activated oxygen) on the other semi-conducting oxide are relaxed by water formation from oxidation of hydrogen. The metallic atoms from the support surface thus act as modifiers to the primary metal particles by the formation of a bimetallic phase. As a result, the electronic configuration of supported metal particles can be modified in a subtle manner which consequently influences the catalytic performance. It is believed this concept of designing nano-hetero-junction empowers scientists to approach new catalytic reactions in a systematic manner, allowing fine-tuning of catalysts with superior performance.

1. Introduction

Semi-conductor usually plays a critical role in catalysis reactions since most of the working catalysts involve semi-conductor component(s), particularly in the form of metal oxide(s) as support material.[1] The catalytic properties of semi-conductor are strongly related with its band structure which can be well-tuned by several methods, doping, hetero-junction, hybridization, morphology control, to name but a few examples.[2,3] Introducing another semi-conductor modifier to establishing a hetero-junction with a specific energy level alignment is one of the simpliest methods for structure tuning, due to a wide range of choices of modifiers and well-acquired skills for their syntheses. In fact, hetero-junction is thought to be commonly established in multicomponent catalysts which are composed of differrent phases of different electronic energy levels. For example, TiO_2 is widely used in photo-catalysis and in solar cell. The photo efficiency is severely limited by its large band gap energy of 3.2 eV, which restricts its absorption in the visible-light region.[4,5] The appropriate introduction of other semi-conductor metal oxides, *e.g.* CeO_2, Co_3O_4 and Cu_2O, not only improves the thermal stability of TiO_2 structure but also effectively extends the photo-response to the visible light region.[6] Cu based catalysts are well known for methanol synthesis from synthesis gas, which has been studied for many years. Semiconducting ZnO is commonly used as the main catalyst component, while the addition of other semi-conductor oxides such as Al_2O_3, Ga_2O_3, ZrO_2, *etc.*, are widely reported to promote the catalytic activity.[7,8] Although the reaction mechanism is still not clear despite many years of intense debates, the establishment of hetero-junction interfaces in this multi-component catalyst is attracting increasing attentions.

A hetero-junction is defined as a materials interface of two layers or two regions of different crystalline semi-conductors. Opposed to a homo-junction, these semi-conducting materials have unequal band gaps. There are at least three types of hetero-junctions, as illustrated in Figure 1: straddling gap (type I), staggered gap (type II) and broken gap (type III).[9,10] For type I, the conduction band of semi-conductor 1 is higher than that of semi-conductor 2 while the relative energy level is opposite in the valence bands. In type II, the band gaps of two semi-conductors are similar but not at the same band energy positions, hence creating staggered bands.[11-13] In type III, the band energy levels of two semi-conductors simply do not overlap at all.

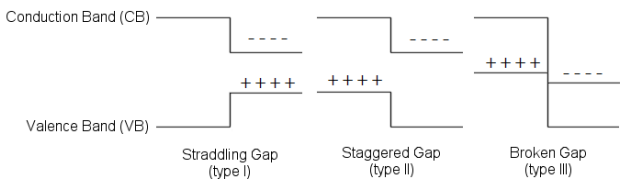

Figure 1. The relative energy levels of semi-conductors for the three types of hetero-junctions. (Note that semi-conductor 1 locates on the left while semi-conductor 2 on the right)

For typical semi-conductors, some thermal- or photo- 'excited electrons' could momentarily overcome the forbidden band gap

[a] F. Liao, T. W. B. Lo, Prof. S.C.E. Tsang
Wolfson Catalysis Centre, Department of Chemistry
University of Oxford
Oxford, OX1 3QR, UK
E-mail: edman.tsang@chem.ox.ac.uk

and occupy the higher energy conduction band.[14] Simultaneously, activated holes are left in the valence band. The catalytic properties of semi-conductors mainly originate from these generated electrons and holes from excitation, since these carriers can be extremely active in redox reactions if sufficient lifetime is established. The electrons in the conduction bands act as strong reductants, while the holes in the valence bands as oxidants. However, a majority of these excited carriers actually recombines rapidly in a single phase semiconductor either radiatively or non-radiatively as heat, which significantly limits the catalytic ability.[14] On the other hand, by using at least two semiconductors, from the energy levels alignment of three types of hetero-junctions as described above, the carriers are confined in semi-conductor 2 for type I.[10] As to type II, the electrons and holes are spatially seperated across the interface and are localized on different sides of the hetero-interface, as shown in Figure 1. Thus, the polarization of two carriers over two semiconductor materials at the interface is taken place at the type II hetero-junction.[9] Due to the spatial separation of electrons and holes, the lifetime of excitons in type II hetero-junction is usually longer compared to that of type I, type III or their single phases. This allows more involvements of these carriers in catalysis processes before their recombination. As a result, some novel properties are usually observed in type II hetero-junction compared with other junctions. Therefore, this mini-review mainly focuses on the applications of type II hetero-junction in catalysis and corresponding catalytic mechanisms.

2. Characterizations

2.1. Powder X-ray diffraction (PXRD)

PXRD is one of the most commonly used characterization techniques to identify the crystalline phase of materials. In hetero-junction, multiple phases of semi-conductors co-exist, therefore diffraction patterns of indivdiual phases are simultaneously observed. For example, our group have synthesized a series of ZnO-CdX (cadmium chalcogenide, X=S, Se, Te) nano-hetero-junctions with introduction of minor CdX phase into bulk phase of ZnO. As shown in Figure 2, the main diffraction pattern of ZnO and minor CdX pattern are clearly observed at the same diffractogram, indicating the co-existence of CdX and ZnO phases in the materials.[15] However, identifying separated phases in nano-hetero-junctions faces a number of challenges. Firstly, when the size of crystalline phase is smaller than 4 nm, it is rather difficult for PXRD to distinguish the mixed phases in nano-hetero-junction structures due to the severe line broading effect of PXRD. The broadening of the diffraction peaks of nano-materials with the decreasing of particle size usually causes overlapping of diffraction patterns from different phases. Improved X-ray monochromation particularly the use of synchrotron and advance instumentation[16a] and the use of multiple peak fitting algorithm[16b] may resolving the diffraction peak overlaps. Secondly, the structural deformation (lattice strain) of mixed nanosize phases as core-shell or Janus paritcle morphologies[16c] could cause a significant shift of diffraction peak position, making the identification process difficult. Thirdly, the structural alteration of materials in nano-dimension and variation in defects[14] can also affect the mixed phases identification.

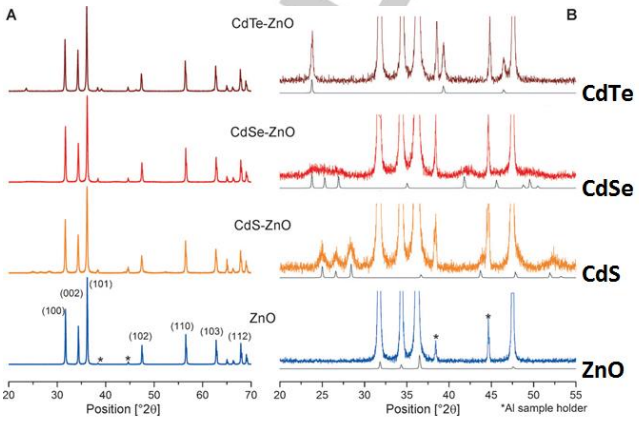

Figure 2. PXRD patterns of ZnO-CdX (X=S, Se, Te) nano-crystal ensembles: A) full spectra showing intense wurtzite-ZnO reflections; B) Expanded portion of spectra showing less-intense, broader wurtzite-CdS, wurtzite-CdSe, and zinc blende-CdTe peaks.[15]

2.2. Transmission electron microscopy (TEM) and selected area electron diffraction (SAED)

TEM is a powerful technique used to observe working catalysts at nano-scale directly, which reveals important information about the finest details of the internal structure, including particle size, morphology and atom arrangement, *etc.* of a particular solid phase. These internal characteristics of various semi-conductors in a catalyst are usually different. SAED is a crystallographic experimental technique that can be performed inside a TEM that uses the TEM electron beam as the incident beam for diffraction. Therefore, accompanying the acquiring of TEM images, the obtained electron diffraction pattern of the selected nano-area can be used to accurately identify the structure of each crystalline components. Although SAED is subject to the same issue of peak boradening, phase identification problems as the PXRD due to small size of crystalline structure, this technique and the spatial distribution of diffraction spots in projected image could help to analyse a wider diffraction range at higher resolution. Figure 3 shows the nano hetero-junction interface of SnO_2-In_2O_3 reported by Xie *et al.*[16d] Clear spacings of SnO_2 (200), (101) facets and In_2O_3 (222), (011), (200) facets are observed in a small selected area which indicates the intimate contact of the two phases. The corresponding SAED patterns of the composite materials are shown on the right. Two sets of diffraction spots are assigned to SnO_2 and In_2O_3 nano phases, respectively, which can further confirm the co-existence of the two semi-conductors in a selected nano-region.

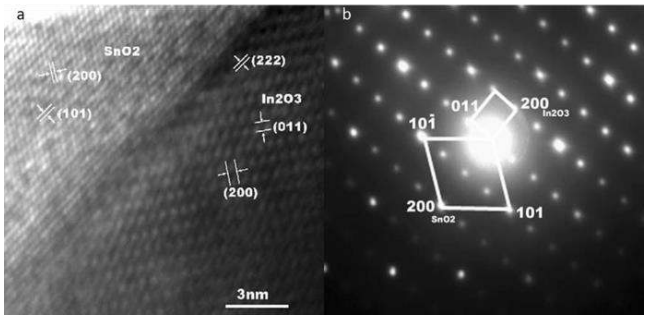

Figure 3. a) High resolution TEM image for the SnO_2-In_2O_3 interface; b) Corresponding SAED of the SnO_2-In_2O_3 composite material.[16]

2.3. Ultraviolet-visible light (UV-vis) diffuse reflectance (or absorbance) spectroscopy (DRS)

UV-vis DRS is also commonly used to characterize the band gap of semi-conductors. With the exposure of a working catalyst to UV-vis light, the photo-energy can be absorbed strongly when the wavelength of the light matches with the band gap width of individual semiconductor component and a sharp absorption edge is observed. According to the position of absorption edge, the value of band gap of a phase can be determined. For hetero-junctions materials, multiple edges should be shown in the DRS. Figure 4 shows the diffuse absorbance spectra of a series of novel g-C_3N_4/Ag_3PO_4 hetero-junction catalysts with variable compositions.[17] With the co-existence of the two phases, two absorption edges at around 400 and 550 nm are observed, corresponding to the electron transitions across the band gaps of g-C_3N_4 and Ag_3PO_4.

However, significantly lower absorption values and lesser sharpness of absorption edges are commonly encountered in nano-hetero-junctions due to larger interfacial contact with atoms exchanged across, which make the phases identification and their differentiation much more difficult to achieve.

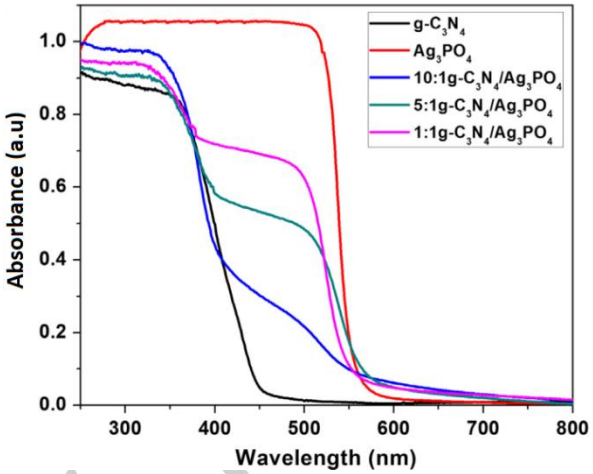

Figure 4. UV–vis diffuse absorbance spectra of pure g-C_3N_4, Ag_3PO_4 and g-C_3N_4/Ag_3PO_4 hetero-junctions.[17]

2.4. Time-resolved photoluminescence (TRPL)

TRPL is a powerful technique to characterize the behavior of excitons in semi-conductors. With the establishment of type II hetero-junction, the electrons and holes (excitons) are separated across the interface of two semi-conductors. As stated in the introduction section, this spatial separation usually prolongs the lifetime of the excitons. This extension can be uniquely detected by TRPL. It is noted that XRD and TEM were unable to distinguish the two nano-phases of $ZnFe_2O_4$ and Fe_2O_3 in nano-hetero-junction of $ZnFe_2O_4$-Fe_2O_3 due to small nanoparticle size with similar crystal structure of $ZnFe_2O_4$ and Fe_2O_3. Excitingly, the significantly enhancement of excitons lifetime in $ZnFe_2O_4$-Fe_2O_3 detected by TRPL can still indicate the type II hetero-junction formation.[14] Figure 5 and Table 1 shows the TRPL and the corresponding fitting results of nano-hetero-junction of $ZnFe_2O_4$-Fe_2O_3 in comparison with pure nano-phases of $ZnFe_2O_4$ and Fe_2O_3. Apparently, the excitons in the nano-composite material with $ZnFe_2O_4$-Fe_2O_3 nano-hetero-junction exhibits much longer lifetime than those of pure phases (Table 1). Thus, this technique which does not subject to the same limitations as diffraction techniques, hence could be used as a technique to probe the nano hetero-junctions.

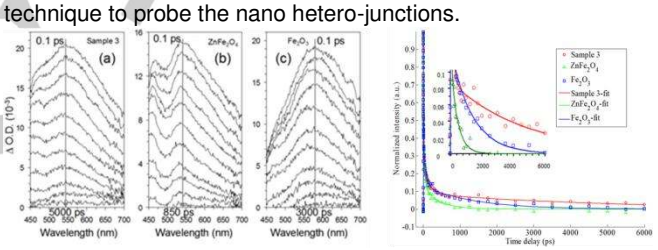

Figure 5. Left) TRPL recorded for (a) sample 3 ($ZnFe_2O_4$:Fe_2O_3=1.0) at time intervals 0.1, 0.2, 0.35, 0.7, 1.75, 6, 15, 50, 250, 1500 and 5000 ps; (b) $ZnFe_2O_4$ at time intervals 0.1, 0.2, 0.35, 0.7, 1.5, 5, 20, 50, 100, 200 and 850 ps; and (c) Fe_2O_3 at time intervals 0.1, 0.25, 0.35, 0.6, 1.5, 6, 17.5, 60, 175, 850 and 3000 ps after excitation at 350 nm in water. Right) Normalized experimental and fitted kinetic decay profiles of photoluminescence at 500-700 nm for sample 3 (○), $ZnFe_2O_4$ (⌜), and Fe_2O_3 (□); the region of 0-0.1 normalized intensity is enlarged in the inserted figure.[14]

Table 1. Time constants (τ) and the associated amplitudes (a) of $ZnFe_2O_4$, Fe_2O_3, and sample 3 ($ZnFe_2O_4$: Fe_2O_3=1.0) measured by TRPL[14]

Sample name	t_{av} ($t_{av}=\tau_i \times a_i$) (ps)	τ1 (ps)/a1	τ2 (ps)/a2	τ3 (ps)/a3	τ4 (ps)/a4
$ZnFe_2O_4$	52.80	0.47/ 0.52	4.74/ 0.15	41.36/ 0.23	423.35/ 0.10
Fe_2O_3	160.94	0.49/ 0.49	7.15/ 0.22	64.24/ 0.18	1341.51/ 0.11
Sample 3 ($ZnFe_2O_4$:Fe_2O_3=1.0)	353.64	0.43/ 0.56	8.99/ 0.23	135.41/ 0.14	4748.17/ 0.07

Besides the mentioned PXRD, DRS, TEM and TRPL, other techniques such like electron energy loss spectroscopy (EELS), high-sensitivity low-energy ion scattering (HS-LEIS), atomic probe tomography (APT), *etc.* may also be useful in the hetero-junction characterization but each techniques have their own limitations and the applications are sometimes restricted by availability of equipment in general catalysis laboratories. A combination of a wide range techniques through collaboration is

commonly required to provide a more accurate representation of the interfacial structure(s) of the nano-hetero-junction.

3. Applications of nano-hetero-junction in catalysis

From the viewpoint of excitation source, catalysis reactions can be classified into photo-catalysis and thermal-catalysis. The concept of hetero-junction catalysts is well known in photo-catalysis since semi-conductors with distinctive band gaps are commonly used. They can efficiently absorb light energy to generate excited electrons and holes which are active enough to react with the adsorbed molecules and eventually catalyze the redox reactions.[18] On the other hand, photons are not necessary to be the only excitation energy source. Thermal energy can also promote electrons from valence band to conduction band in semiconductor although it is less specific and the energy transfer is not as efficient as the photonic means. Recently, it was firstly demonstrated by our group that nano-hetero-junction can be applied into traditional thermal-catalysis, particularly, in the metal/metal oxides catalysts which are regarded as the most frequently used catalysts. With the establishment of type II hetero-junction in two semi-conducting support oxides, the reduction behaviors of the semi-conductor supports to corresponding metallic atoms can be rationalized. The produced metallic atoms derived from the support can act as modifier for the primary supported metal nanoparticles and tune its catalytic properties in a subtle manner through the formation of bimetallic species. The typical applications of nano-hetero-junction in these catalytic reactions are reviewed in this section.

3.1. Photo-catalysis

It is well accepted that our present non-renewable energy resources, such as oil, gas and coal, cannot dominate the energy and chemical markets for too long due to their finite reserves and rapid consumption.[19-22] As one of the primary renewable energies in nature, sunlight with abundant supply to many places on earth has become a favorable alternative and is getting increasing attentions.[23] In chemistry, photo-catalysis is the occurrence of a reaction driven by light energy instead of chemical or thermal energy in the presence of a catalyst. The quantized light energy is primarily absorbed by a working photocatalyst that contains semi-conductor(s) through the electron transition process across the band gap provided the wavelength of the light matches in energy with the band gap. The generated electron–hole pairs can be extremely active to react with the adsorbed substrate molecules on the surface of catalyst if their rapid recombination is tamped. This process consumes the surface carriers and subsuquently produces some surface species or radicals. Simultaneously, the light energy is captured and transferred from the catalyst to substrate molecule. Then, the produced species/radicals react with each other and produce products. The whole process is demonstrated in Figure 6. The photocatalytic activity (PCA) in turn of quantum yield of efficiency mainly depends on the ability of the photocatalyst to create electron-hole pairs which is active to generate for example, free radicals (*e.g.* hydroxyl radicals: •OH) to undergo secondary reactions.

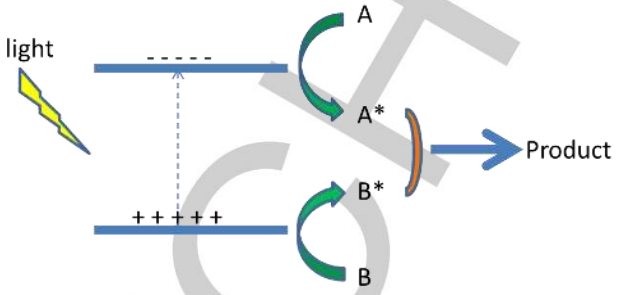

Figure 6. The demonstration of a typical photo-catalysis process.

Comparing with industrial catalytic reactions that often require high temperature and elevated pressure, photo-catalysis operates under basically ambient conditions if an adequate radiation source is available.[18] Currently, the most commonly used materials in photo-catalysis include TiO_2, ZnO, CdS, etc. and various promoters are usually added to optimize the catalytic performance. The applications of photo-catalysis have been mainly focused in the fields of pollution removal using radicals for organics destruction and in energy production involving H_2 production from water.[24-27] The manufacture of useful chemicals by photocatalysis is yet to be explored.

3.1.1 Photo-catalytic H_2 evolution from water decomposition

Hydrogen gas is considered as the cleanest energy carrier.[28-30] However, its large scale production is presently derived from steam reforming of natural gas, which is obviously unsustainable in this non-renewable reserve with a hugh carbon emission probem. Thus, as shown in the following equation, photo-catalytic hydrogen production from water decomposition, particularly with the utilization of visible light, is being regarded as an alternative route to obtain renewable hydrogen.[31]

$2H_2O \rightarrow 2H_2 + O_2$

More frequently sacrificial electron donors such as methanol are used to boost the rate of hydrogen evolution as accordingly[18]:

$H_2O + CH_3OH \rightarrow CO_2 + 3H_2$

Sulphides are found to be the most active photocatalysts components for H_2 evolution and the reported active ones includes CdS, $AgGaS_2$, MoS_2, *etc.* CdS nanoparticles have a narrow and direct band gap (2.3 eV), which is effective for capturing the visible light regime and is greater than 1.23 eV, the minimum energy required for water splitting.[29,32] However, the rapid instant recombination of photo-generated electrons and holes in photo-activated CdS and the high kinetic barrier for hydrogen production on the surface do not allow the direct efficient conversion of solar energy to hydrogen gas.[33] Fortunately, with the addition of appropriate secondary semi-conductors, the catalytic performance can be significantly improved. Li *et al.* reported the the rate of H_2 evolution can be increased by up to 28 times when CdS was loaded with only 1.0 wt% WS_2.[34] The relevant characterizations indicate that the significantly enhanced H_2 evolution of WS_2/CdS catalyst is

mainly caused by the hetero-junctions formed between WS_2 and CdS. The excited electrons generated on CdS can be transferred to the surface of WS_2 which offers a much lower kinetic barrier for the reduction of H^+ to H_2, as shown in Figure 7.

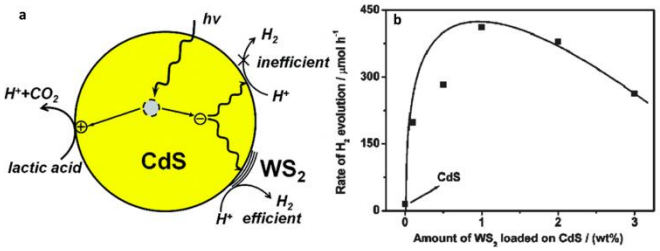

Figure 7. a) Proposed reaction mechanism for photo-catalytic H_2 production on WS_2/CdS catalyst; b) Rate of H_2 evolution on CdS photo-catalysts under visible light (λ > 420 nm) loaded with different amounts of WS_2.[34]

Our group have reported a novel CdS–graphene–MoS_2 catalyst which increased the H_2 yield from water by 70 times.[32] With the co-existence of MoS_2 and graphene, the generated electrons on CdS by the absorption of visible light can be transferred into the conduction band of MoS_2 efficiently through the graphene as electron conductor which decreases the radiative recombination of the carriers. (The staggered energy levels of CdS and MoS_2 are shown in Figure 8.) Meanwhile, MoS_2 provides a much lower kinetic barrier for H_2 evolution than CdS. Thus, this multiple-component photocatalyst accelerates the reaction rate for H_2 production significantly. The proposed catalysis mechanism and catalytic result, are shown in Figure 8 and Figure 9

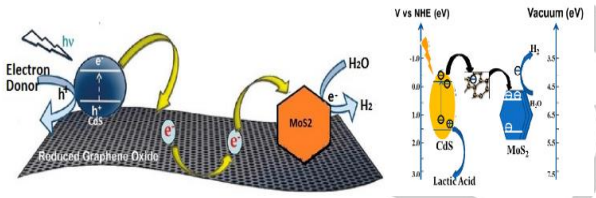

Figure 8. Proposed reaction mechanism of graphene supported CdS and MoS_2 for photocatalytic hydrogen evolution.[32]

Usually, the catalytic performance of hetero-junction catalysts can be further promoted by the addition of a small amount of noble metal, which facilitates the electron transfer at the interface and decreases the instant recombination of excitons. As reported by Li *et al.*, the Pt loaded CdS-PdS system gave a H_2 yield of 29,233 μmol $h^{-1}g^{-1}$ with S^{2-}/SO_3^{2-} as the sacrificial agent.[35] The value was even raised to 40,000 μmol $h^{-1}g^{-1}$ by Alivisato *et al.* in Pt promoted CdS-CdSe system.[36]

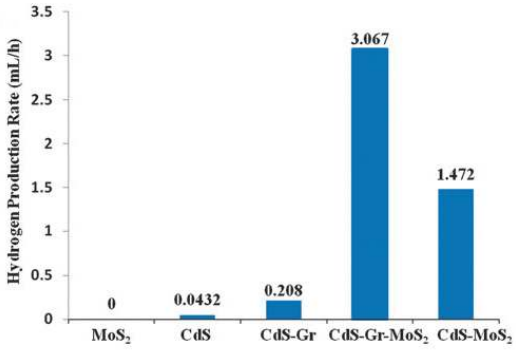

Figure 9. Photo-catalytic hydrogen evolution rates over MoS_2, CdS, CdS–graphene, CdS–graphene–MoS_2 and CdS–MoS_2 (20 mg samples in 10% lactic acid).[32]

3.1.2 Photo-catalysis in solar cell

In term of sunlight conversion into utilisable energy, photo-catalytic production of H_2 is perhaps of less desirable due to an extra step required to convert produced H_2 into electrical energy (PEM fuel cell and combustion engine). More importantly, the time scale for recombination of photogenerated excitons of typical semiconductor (< 10^{-10} s) is generally much faster than chemical reactions (10^{-10}-10^{-5} s) despite the use of hetero-junction. In contrast, charge separation can be rapidly achieved by using electromotive force in an external circuit. Thus, the investigation of solar cell for capture of sunlight is currently one of the most intense research themes. Solar cell is an device that converts light energy directly into electricity by photovoltaic effect.[37-40] The operation of a photovoltaic (PV) cell requires three basic attributes:

i. The absorption of light, generating electron-hole pairs.
ii. The separation of charge carriers of opposite types.
iii. The extraction of those carriers to an external circuit.

Therefore, semi-conductors components are essential for solar cell devices due to the intrinsic characteristics of semi-conductors, the discrete band structures, the transition of electrons across the band gaps, etc. Type II hetero-junction has been confirmed to be an effective method to increase the energy efficiency, since it helps to keep separation of charge carriers and allows their extraction to an external circuit. Silicon is a hot topic in crystalline silicon photovoltaic as it allows solar cells with energy conversion efficiencies above 21%, also at industrial production level.[41] These Si based solar cells consist of thin amorphous hydrogenated silicon (*a*-Si: H) layers on monocrystalline silicon wafers (*c*-Si wafer), as shown in Figure 10a. The amorphous silicon is easily doped to be either negative type (*n a*-Si: H) or positive type (*p a*-Si: H), Therefore the band gap of this type silicon can be well-tuned. With a few layers of deposition of two types amorphous silicon deposited on the two side of bulk crystalline silicon, a type II hetero-junction can be established which enhances the spatial separation of the carriers of opposite charge through charge transfer across the hetero-junction interface, as shown in Figure 10b. As stated, the energy conversion efficiency of this type solar cell can reach over 20%.

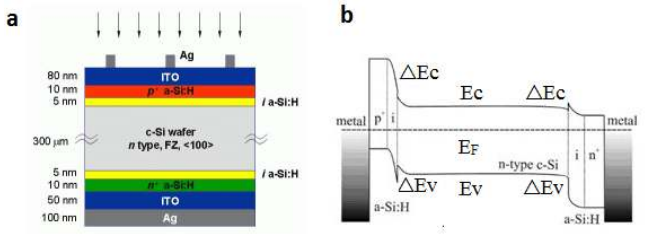

Figure 10. a) Schematic diagram of a hetero-junction solar cell (drawn not to scale); b) Electronic band diagram of a hetero-junction solar cell (drawn not to scale).[41]

Besides silicon, CdTe is another leading material for the development of cost effective solar cell. The two key properties of this semi-conductor are its near ideal band gap for visible light absorption of 1.45 eV, and its high optical absorption coefficient.[42] CdS is usually added to establish a type II hetero-junction to increase the carrier separation efficiency. As reported by Morales-Acevedo *et al.*, a system of thin film of polycrystalline CdSe-CdS exhibited a high energy conversion efficiency of 16.5% which was almost the calculated theoretical limit of this system under visible light irradiation (400 - 850 nm).[42]

Recently, it was reported that the one-dimensional (1-D) structure of nano-wires or nano-rods serves as direct pathway for the transportation of carriers in solar cell and the efficiencies have been increased significantly compared to the nanoparticles or the porous versions.[43-44] As a result, the decoration of cadmium chalcogenide (CdX) quantum dots (QDs), namely, CdS, CdSe and CdTe, on arrays of ZnO rods or wires is under extensive research due to the formation of type II CdX-ZnO hetero-junction and the direct transportation pathway of 1-D ZnO for electrons. Wang *et al.* aligned ZnO/CdTe core–shell nano-cable arrays on an indium tin oxide (ITO) substrate and constructed a photoelectrochemical device with a photocurrent of 5.9 mA cm^{-2} (at 0 V vs Ag/AgCl) which was much higher than that of anode without CdTe decoration (less than 1.0 mA cm^{-2}).[45]

Li *et al.* reported the design and characterization of novel double-sided CdS and CdSe QD co-sensitized ZnO nano-wire arrayed photo-anodes for photo-electrochemical (PEC) hydrogen generation.[46] The TEM images are shown in Figure 11. These photo-anodes exhibit strong absorption in nearly the entire visible spectrum up to 650 nm, with a high incident-photon-to-current-conversion efficiency (IPCE) of ~45% at 0 V vs Ag/AgCl which were much higher than that of pure ZnO photo-anode. The observed linear sweep voltammograms and the proposed electron pathway are displayed in Figure 11B and Figure 12. The formation of type II hetero-junction helps the separation of carriers and the 1-D structure of ZnO wire promotes the transferring efficiency of electrons to the copper wire. Most recently, the PbI_2 perovskite based solar cells with the establisment of efficient heterojunctions are currently under intensive research as a Si alternatives to reduce the prime cost. The energy conversion efficiencies are comparable with that of Si-based solar cell but the materials are much cheaper.[47]

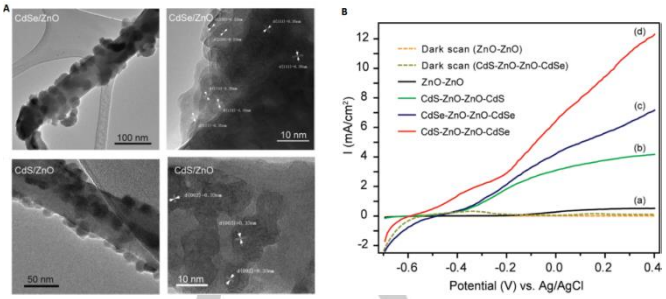

Figure 11. A) TEM images of ZnO NW sensitized by QDs. Low-resolution (left column) and high-resolution (right column). TEM images of (top) CdSe QD-sensitized ZnO NW and (bottom) CdS QD-sensitized ZnO NW. White lines highlight the measured lattice spacings in the TEM images, which are corresponding to the d-spacings of CdSe and CdS. B) Linear sweep voltammograms of photo-anodes fabricated from (a) ZnO-ZnO, (b) CdS-ZnO-ZnO-CdS, (c) CdSe-ZnO-ZnOCdSe, and (d) CdS-ZnO-ZnO-CdSe nano-wires at a scan rate of 10 mV s^{-1} at applied potentials from -0.7 to +0.4 V, under a light intensity of 100 mW cm^{-2}.[46]

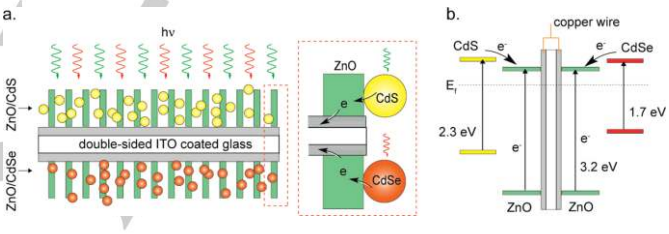

Figure 12. Schematic diagrams illustrating (a) the architecture and (b) the corresponding energy diagram of double-sided CdS-ZnO-ZnO-CdSe NW arrayed photo-anode. The dashed box highlights the CdS-ZnO and CdSe-ZnO interfaces.[46]

3.1.3 Photo-catalytic decomposition of aqueous organic molecules

With the rapid development of economy and increasing population, the waste released from human activity into the global water, such as heavy metals, solvents and toxic sludge, have reached 300 – 400 million tons per year.[48] These pollutants impose a great environmental pressure, particularly the hazardous organic molecules.[48] Meanwhile, new recalcitrant organic pollutants are continuously emerging and released into the environment. As a result, the development of new facile methods to obliterate these contaminants is urgently desired.

Photo-catalytic oxidation of organic pollutants has been considered as a promising technique where the toxic material is usually oxidized to harmless CO_2 and H_2O.[49-52] During these processes, the contaminants are degraded mainly by the attack of OH• or O_2• radicals which are produced from the excitation of photo sensitive catalysts, as shown in Figure 13;[53-55] the photo-generated electrons and holes on the surface of catalyst is active to react with O_2, H_2O, OH^- in the system to generate OH• and O_2• radicals.

Among a wide variety of semi-conductors, TiO_2 has been regarded as a promising environmentally friendly photo-catalyst due to its biological and chemical inertness, as well as the strong oxidizing power originating from the position of its valance and conduction bands. Meanwhile, TiO_2 is cheap and stable against photo and chemical corrosion, which also makes it outstanding among a wide range of semi-conductor photo-catalysts.[56-60] Unfortunately, the rapid electron-hole pair recombination of this semiconductor oxide generally leads to its very low photo-catalytic efficiency.[61,62] In addition, the band gap of TiO_2 is usually over 3 eV (3.0 - 3.5 eV). This wide band gap significantly limits the utilization of sunlight as the infrared and visible light (with energy of less 3.2 eV) contributes 95% of the energy of the sunlight spectrum. It has been proved that building hetero-junctions can efficiently tune the band structure of TiO_2 based catalysts and separate the carriers (electrons and holes) across the components interfaces. Jin *et al.* reported that even a mixture of rutile/anatase TiO_2 hetero-junction with uniform chemical composition can significantly promote the photo-catalytic ability in the degradation of methyl blue (MB).[63] The enhanced performance was assigned to the staggered energy levels of rutile and anatase TiO_2 which separated the photo-generated electrons and holes on the surfaces of rutile and anatase, respectively. This spatial separation prolongs the lifetime of the carries, which consequently promotes the formation of active O_2• and OH• radicals and accelerates the secondary reactions. The similar enhancement was also observed in a CeO_2-TiO_2 hetero-junction system reported by Liu *et al.*[64] With the surface decoration of CeO_2 nano-particles, the catalytic ability of TiO_2 rods in the degradation of rhodamine B (RB) solution was raised to 6 times due to the better separation of photo-generated electrons and holes. To increase the utilization efficiency of visible light, Shi *et al.* added some $CoFe_2O_4$ and polyaniline to modify the optical properties of TiO_2 catalyst.[65] The catalytic performance of this ternary catalyst was strongly promoted under visible light due to the formed hetero-junction of added polyaniline with TiO_2, which promoted the electron-hole separation, as shown in Figure 14a. $CoFe_2O_4$ was introduced to facilitate the charge transfer across the interface of polyaniline-TiO_2 phases particularly for the holes in the conduction bands since the energy gap between polyaniline and TiO_2 is too wide (Figure 14a). Simultaneously, the addition of $CoFe_2O_4$ also increased the energy absorption in visible light range owing to the relatively narrower band gap around 2.0 eV compared with that of 3.5 eV in TiO_2.

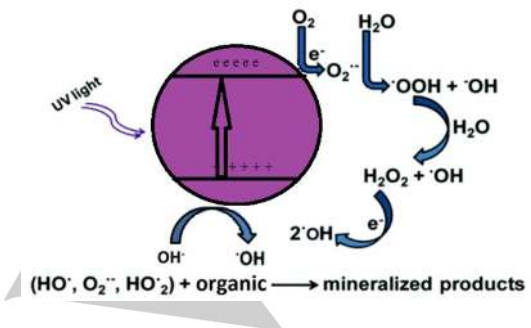

Figure 13. The formation mechanism of radicals on semi-conductor catalyst under light irradiation.

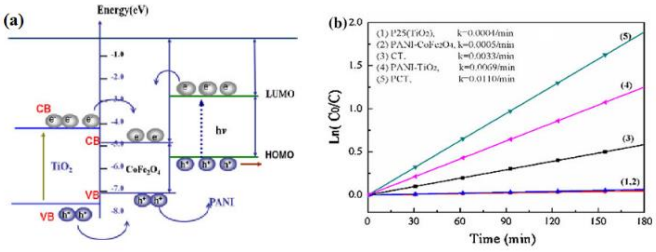

Figure 14. a) Possible charge transfer of polyaniline-$CoFe_2O_4$-TiO_2 (PCT) catalyst; b) the Plots of degradation of MB over different samples under visible light irradiation; (1) TiO_2 (2) polyaniline-$CoFe_2O_4$ (3) $CoFe_2O_4$-TiO_2 (4) polyaniline-TiO_2 (5) polyaniline-$CoFe_2O_4$-TiO_2.[65]

Besides TiO_2, ZnO is another widely studied material for the photo-decomposition of organic pollutants and toxic contaminants in air and water.[66-69] However, similar to TiO_2, the realization of high catalytic performance is limited by the fast internal excitons recombination caused by the wide band gap (3.2 eV). Several approaches have been investigated to improve ZnO catalytic activity, including both cation[70] and anion[71] doping, metal–semi-conductor Schottky junctions,[72-74] surface decoration with organic molecules,[75] and morphology manipulations.[76,77] Besides these, the creation of multiphase or "heterostructured" semi-conductor systems is regarded as an effective way. To date, most of the synthesis of these systems deposited a second semi-conductor phase onto pre-formed ZnO nano-crystals (NCs). Jaegermann *et al.* reported a novel SnO_2−ZnO hetero-junction consisting of a mesoporous network of aggregated wurtzite ZnO decorated by cassiterite SnO_2 nano-crystallites, which showed much higher photo-catalytic activities for the degradation of MB than those of individual SnO_2 and ZnO nanomaterials, as indicated by the rate constant values in Figure 15a.[78] After the determination of band structure of the catalyst, the enhancement was assigned to the formation of SnO_2-ZnO hetero-junction, as shown in Figure 15b.

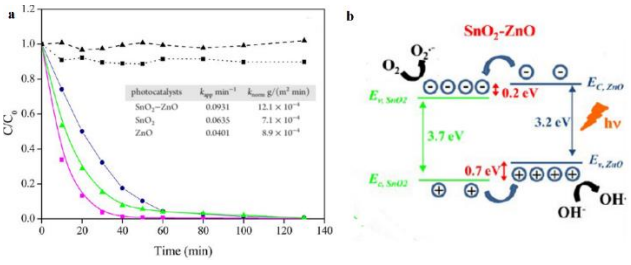

Figure 15. a) Kinetic of the degradation of MB in the presence of UV only (square, dot), SnO_2−ZnO in the dark (triangle, dash), SnO_2−ZnO under UV (square, plain), SnO_2 under UV (triangle, plain), and ZnO under UV (circle, plain); inset shows the calculated rate constant of MB degradation, k_{app} represents the apparent rate constant while k_{norm} is the rate constant normalized by BET surface area. b) Mechanism of radical generation catalyzed by SnO_2-ZnO hetero-junction.[78]

Similar enhancements have been observed in ZnO/CdSe,[79] ZnO/CuS,[80] ZnO/CdTe[81] and ZnO/CdS[82] systems. Although the type II hetero-junction effect has been observed in several photo-catalytic systems, the detailed investigation in the relationship of catalytic ability with nano-junction structure of catalyst has not been reported. Meanwhile, the decoration of a secondary semi-conductor modifier on the ZnO surface exposes the modifier with narrow band gap into the reactants which usually leads to a photo-corrosion to the catalyst and causes catalyst deactivation. For the first time, our group reported a series of high quality hetero-structured photo-catalysts prepared by growing ZnO nano-crystals (NCs) around pre-formed cadmium chalcogenide quantum dots (QDs) using a simple and scalable solution-based approach.[15] We demonstrated the successful growth of ZnO tetrahedrons around colloidal CdS, CdSe, and CdTe quantum dots (QDs), which gave rise to novel type II hetero-structured semi-conductor nano-crystals (HSNCs) with significantly increased photo-catalytic activity relative to pure ZnO. In performing a comparative study across a series of chalcogenides, we observed that the rate of exciton generation, and hence photo-catalytic activity, was related to both the nature of the chalcogenide anion (X^-) and the structure of the junction between the different semi-conductors. The use of atomic probe tomography (APT) to characterise these hetero-junctions yielded unprecedented insights into the nano-hetero-junction structure, which revealed the increasing degree of interfacial atoms exchange (CdS<CdSe<CdTe) proportional to the materials softness and inversely proportioned to their lattice mismatch. We also observed that CdS and CdSe NCs can form extensive but sharp material interface with ZnO crystals while the much softer CdTe NCs with highest lattice mismatch generated more extensive atoms exchange with ZnO, leading to total encapsulation by the ZnO crystalline phase. Thus, the establishment of an internal CdTe/ZnO nano-interface promoted the photo-catalytic properties of ZnO without photo corrosion of CdTe. The corresponding catalytic results of the series of materials, TEM and APT are shown in Figure 16, Table 2 and Figure 17, respectively. The core-shell structure of CdTe-ZnO NCs shows the highest catalytic ability due to the strongest interaction of CdTe and ZnO (as shown in Table 2, the band gap of ZnO in the core-shell structure lowers to 3.21 eV, while CdS and CdSe show much less significant effect.)

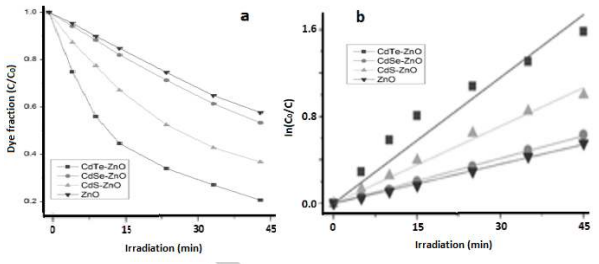

Figure 16. a) MB decomposition curves under UVA irradiation (l=350 nm); b) Linear plots of pseudo-1st order rate equation. C_0=initial dye concentration.[15]

Table 2. Photo-catalytic rate constants (k-values) and band-gap values (Eg) for HSNCs and pure ZnO.[15]

Catalyst	k value (min^{-1})	ZnO E_g (eV)	CdX E_g (eV)
CdTe/ZnO	$0.039 \pm 2.3*10^{-3}$	3.21±0.04	1.52
CdSe/ZnO	$0.014 \pm 1.4*10^{-4}$	3.26±0.04	1.93
CdS/ZnO	$0.024 \pm 6.2*10^{-4}$	3.26±0.04	2.59
ZnO	$0.012 \pm 1.9*10^{-4}$	3.28±0.03	N.A.

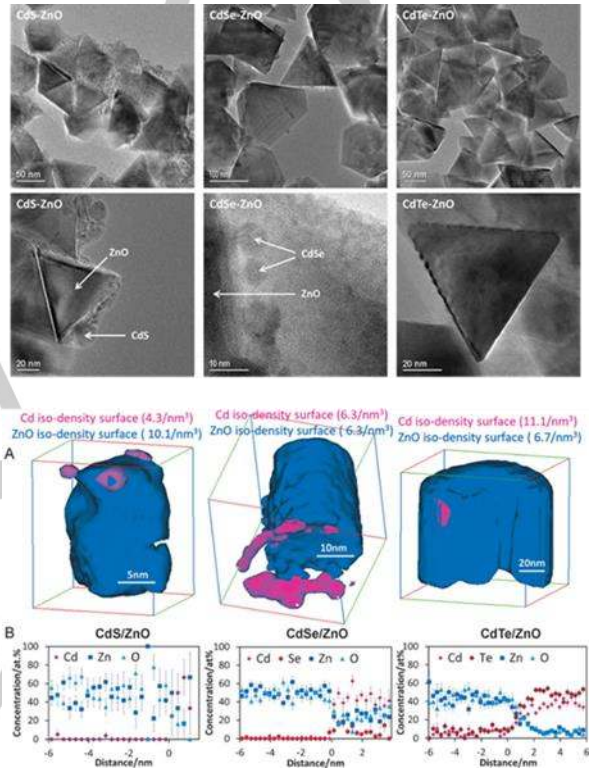

Figure 17. Top) TEM of CdX/ZnO (X=S, Se, Te) HSNCs showing CdS (left) and CdSe (center) decorating the surface of ZnO tetrahedrons, while CdTe (right) is fully encapsulated by ZnO. Bottom) (A) APT three-dimensional spatial reconstruction of Cd^{2+} (pink) and Zn^{2+} (blue) ions present in HSNCs; (B) Atomic composition profile of HSNC nanojunction as a function of scanned distance. (at%=atom%.)[15]

3.2. Thermal-catalysis by nano-hetero-junction

Although the concept of nano-hetero-junction has been applied into the photo-catalysis area for several decades, it is scarely discussed in traditional thermal-catalysis. On the other hand, many traditional catalysts contain finely divided noble metal nanoparticles on a semiconducting transition metal oxide support promoted with other ingredients.[83] In addition, the thermal-catalytic reactions, usually involving the use of high temperature and high pressure during catalysis, which provide the energy input for the material excitation. In the past few years, our group have focused on the establishment of electronic nano-hetero-junction in catalyst support that can effectively tune the thermal catalytic properties of the dispersed noble metals.

Cu/ZnO catalyst is a typical example for the illustration. Due to the primary greenhouse effect of CO_2, catalytic conversion of CO_2 with H_2 to methanol or other condensable valuable chemicals has a positive impact on this important environmental issue.[84,85] The majority research on catalytic studies for CO_2 hydrogenation has used modified industrial methanol catalysts for synthesis gas (CO/H_2) hydrogenation, which contains Cu/ZnO as the main components together with Al_2O_3 as support and with different modifiers.[86-88] However, the commercialization of methanol synthesis from CO_2 hydrogenation is limited by the low methanol selectivity over this catalyst due to the simultaneous rapid formation of CO through reversed water gas shift reaction. Our group reported the synthesis of a novel Cu/CdSe@ZnO catalyst which showed a dramatic promotion of methanol selectivity from 40% of the undoped sample to about 75%, dependent on the CdSe content (Figure 18a).[79] The enhancement was assigned to the enrichment of electron density in ZnO by encapsulating CdSe (electron rich QD) into the ZnO rod through an establishment of the type II hetero-junction. As shown in Figure 18b, the excited electrons by light or thermal energy are accumulated on the surface of ZnO, while holes take residence on CdSe due to the staggered energy levels created at the junction. Figure 19 shows the electron paramagnetic resonance (EPR) signals of ZnO in CdSe@ZnO and pure ZnO phase; apparently, the number of electrons in ZnO conduction band is raised several times by the addition of CdSe, which confirms the excited conduction electrons have been transferred from CdSe and accumulated in ZnO. By mixing Cu nano-particles with ZnO-CdSe support, the accumulated electrons with enhanced electronic potential were transfered to the Cu surface whcih could significantly modify the electronic interaction(s) between Cu site and the reactants. Thereby, the methanol selectivity increases with the concentration of CdSe QD embedded in ZnO rod, as shown in Figure 18. The core-shell structure also minimizes the exposure of CdSe QD to the reactant molecules, which thus avoids its poisoning to the Cu surface

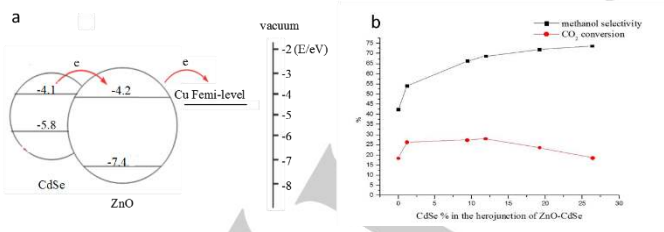

Figure 18. a) Electronic interaction of ZnO, CdSe and Cu at hetero-junctions; b) Influence of CdSe content on the CO_2 conversion and methanol selectivity of the synthesized catalysts.[79]

Since Cu nanoparticle was added to the support by physical mixing, the interaction of CdSe-ZnO and the metallic Cu has not yet been maximized. This present Cu/CdSe@ZnO system is thus only serving as a material model to illustrate the influence of hetero-junction effect in support to the overlying metal particle in thermal catalysis. Another class of hetero-junction catalysts for thermal-catalysis has been studied. Rh/ZnFe2O4-Fe2O3 (or Pd/ZnFe2O4-Fe2O3) hetero-junction catalyst was prepared by co-precipitation method to extensively investigate the interaction of support and dispersed noble metal with intimate contact.14 The electron energy loss spectroscopy (EELS) mapping, EPR and TRPL characterization results confirmed the existence of type II ZnFe2O4-Fe2O3 hetero-junction in the support. It was interesting to observe that the reduction of Fe(III) in the support to metallic Fe(0) by H2 was significantly promoted by the establishment of this hetero-junction and the amount of produced Fe(0) was determined by the ratio of ZnFe2O4 : Fe2O3. For the metal/metal oxide catalyst with intimate interface, it is becoming clear that one of the important interactions is the decoration of supported metal particles with trace reactive metallic elements derived from the support as bimetallic species. The metallic atoms from support is reduced by the activated atomic hydrogen from the metal site which is spilled to the neighboring support oxide. By the introduction of type II hetero-junction, our group demonstrated that Rh (or Pd) noble metal nano-particles can be decorated with controlled amount of reactive Fe atoms to form bimetallic RhFe or PdFe nano-particles with tunable composition by catalytic reduction of ZnFe2O4-Fe2O3 support materials (at a temperature lower than 200 oC). The proposed reduction mechanism is shown in Figure 20; with the formation of ZnFe2O4-Fe2O3 hetero-junction, more holes in terms of activated oxygen species are accumulated on the surface of ZnFe2O4. When noble metal is in proximity, these activated oxygen species (holes) could then react with the spilled atomic hydrogen (produced on noble metal surface) at the interface to form water as their lifetime constant of excitons is comparable to that of this chemical reaction.

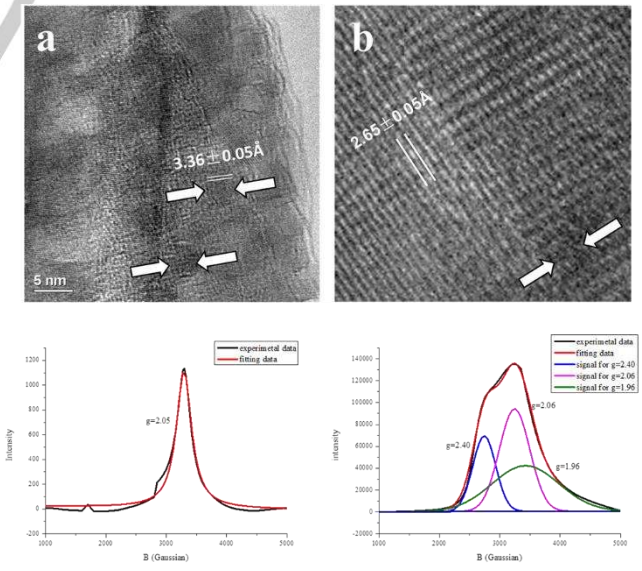

Figure 19. (top) a) HRTEM image of CdSe@ZnO to show embedded CdSe nanoparticles with observed [002] fringes of 3.36 ± 0.05 Å; b) HRTEM on materials interface showing regions of wriggled [101] fringe lines of ZnO. (bottom). Resolved integrated EPR signal of left).~17 mg ZnO rod and right). 40 mg CdSe-ZnO sample (CdSe 26.4 wt%).[79]

Thus, the corresponding electrons in Fe_2O_3 phase will reduce metal ions Fe(III) from the support mixture to metal atoms Fe(0). The number of first shell neighbor Fe to Rh (NFe=5.2) varies with ratio of $ZnFe_2O_4$: Fe_2O_3 in the support as sample 3 ($ZnFe_2O_4$: Fe_2O_3=1.0) > sample 2 ($ZnFe_2O_4$: Fe_2O_3= 0.6) > sample 4 ($ZnFe_2O_4$: Fe_2O_3=8.6) > sample 1 ($ZnFe_2O_4$: Fe_2O_3=0) reflecting the varied composition of RhFe nano-particles by the amount of hetero-junction interface in support. The content of Fe in the bimetallic phase increases with the amount of $ZnFe_2O_4$-Fe_2O_3 hetero-junction interface and reaches the optimum at $ZnFe_2O_4$: Fe_2O_3 =1.0 which has the maximum hetero-junction interface (Figure 21a). Due to the strong interaction of iron oxide based support with the noble metal containing phase, extremely small PdFe or RhFe particles with tunable compositions can be maintained, which exhibit high catalytic ability (as shown in Figure 20b, the average size of Rh containing phase is around 1.5 nm). Meanwhile, the catalytic properties of noble metals can be rationally tuned by varying the composition of the formed bimetallic nano-particles through the electronic interaction with modifier atoms. As shown in Figure 21b, the binding energy of Rh changes with the content of Fe(0) in the bimetallic RhFe nanoparticles indicating the tunable electronic structure of Rh. The catalytic performance of the series of prepared RhFe and PdFe nanoparticles prepared by this $ZnFe_2O_4$-Fe_2O_3 hetero-junction method in the hydrogenolysis of ethylene glycol are shown in Figure 22. The results vary with the content of Fe, corresponding to the amount of $ZnFe_2O_4$-Fe_2O_3 hetero-junction interface. We believe such a fine control in electronic and structural modifications in supported bimetallic catalysts enabled by designed hetero-junctions empowers scientists to approach new catalysis reactions in systematic manner, and allows fine-tuning of catalysts with superior performance for important reactions. It is anticipated that this method may have a potential to identify new catalysts to meet the growing demands for greener catalysts.

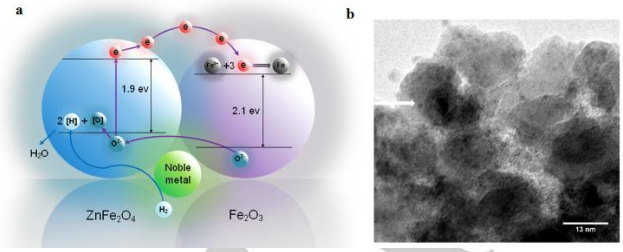

Figure 20. a) Proposed electron flow cycle in the reduction process of two semi-conductor supports catalyzed by noble metal; b) TEM image of reduced Rh/$ZnFe_2O_4$-Fe_2O_3 sample ($ZnFe_2O_4$-Fe_2O_3=1.0).[14]

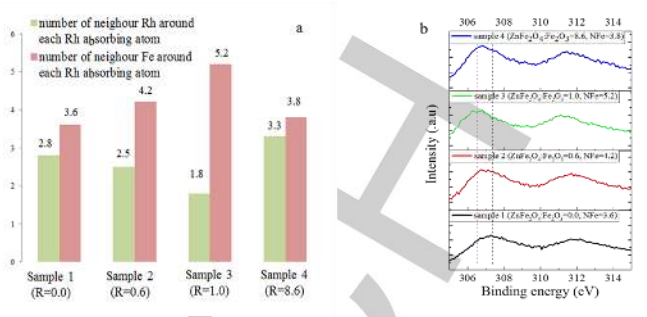

Figure 21. a) Number of neighbor Rh (NRh) and Fe (NFe) atoms around Rh absorbing atom derived from EXAFS fittings; b) Rh 3d XPS curves for samples 1-4 after pre-reduction. R represents the ratio of $ZnFe_2O_4$: Fe_2O_3.[14]

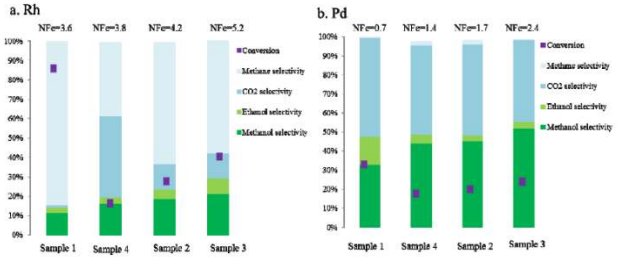

Figure 22. Catalytic performances of (a) Rh samples and (b) Pd samples in hydrogenolysis of ethylene glycol (50 bar H_2, 250 °C, the trace products include CO, C_2H_6, *etc.*).[14]

4. Conclusions

Semi-conductors act as excellent catalysts or catalyst supports in a large variety of important industrial reactions, which range from photo- to traditional thermal-catalysis reactions. By incorporating an appropriate secondary semi-conductor into a working catalyst, a type II hetero-junction in the catalyst can be established. With the excitation of catalyst by light or heat, the generated excited electrons and holes are separated on different phases of the semi-conductors. This hetero-junction effect significantly prolongs the lifetime of excitons, which tunes the catalytic properties.

In photo-catalysis, the photo-generated electrons and holes are the key for the occurrence of chemical reactions or for the generation of photo-current. But the efficiency of excitons utilization is strongly restricted by the instant recombination of electrons and holes. The prolonged lifetime of excitons by hetero-junction effect reduces the recombination of holes and electrons by separating the two on different crystalline phases at the interface. As a result, more electrons and holes with prolonged lifetime can be involved in chemical reactions or be transferred into the electronic device. Clearly, the longer timescale for catalytic reactions would demand a more efficient hetero-junction to prolong the excitons lifetime in converting photon energy to chemical product.

In traditional thermal-catalysis, the mixed phase of semi-conductor oxide as support is commonly used to host noble metal particles. The formed type II hetero-junction in support by blending another semiconducting support material can enhance spatial charge separation hence altering the electronic potential and adsorptive properties of overlying noble metal particles. The hetero-junction can also effectively control the reduction behavior of the semi-conductor oxides to their metallic state, and consequently tune the amount of produced metallic atoms. These atoms with controlled amount from the support phase act as modifiers for the dispersed noble metal nano-particles through the formation of bimetallic phase. They can be in form of core-shell or Janus morphology with adjustable dimensions. As a result, the electronic structure of noble metal can be well tuned in a subtle manner by varying the content of modifiers through the strong electronic interaction of the two elements.

Currently, the research of nano-hetero-junction is mainly focused in the area of photo-catalysis, including the development of solar cell, photo-degradation of environmental pollutants and the renewable H_2 production. The mechanism is clear and some processes have been commercialized. Our group have demonstrated that the hetero-junction effect is also effective in traditional thermal catalysis and the results appear to be promising. Although it is hard to accurately determine the precise role(s) of hetero-junction in thermal reactions due to the complexity of multi-component catalysts, delicate pretreatments of catalysts and applications of extreme temperature and pressure in industrial applicable conditions, we believe the application of nano-hetero-junction concept is a simple and effective way in tuning the catalytic performance of catalysts in a rational manner. Due to the large share of traditional thermal-catalysis in industry, this rational guide of catalysts is extremely important and warrenty further study.

Acknowledgements ((optional))

We wish to acknowledge the finance support from the EPSRC, UK and Oxford University to some of the studies mentioned in this mini-review article.

Keywords: nano-hetero-junction, electron-hole pair, spatial separation, lifetime, band structure

References:

1.S. D. Jackson and J. S. J. Hargreaves (Eds), *Metal oxide catalysis*, *Wiley-VCH,* Weinheim, **2009**.
2. A. M. Smith, S. Nie, *Acc Chem Res*. **2010**, 43(2), 190–200.
3. L. Yin, Y. Bando, *Nat. Mater*. **2005**, *4*, 883–884.
4. X. Chen, S. Mao, *Chem. Rev*., **2007**, 107, 2891-2959
5. A. Fujishima, X. Zhang, D. Tryk, *Surf. Sci. Rep*. **2008,** 63, 515-582
6. T. Cao, Y. Li, C. Wang, L. Wei, C. Shao, Y. Liu, *J. Sol-Gel Sci. Technol*. **2010**, *55*, 105–110.
7. S. Derrouiche, H. Pernot, C. Louis, *Chem. Mater*. **2012**, 24, 2282 – 2291
8. I. Kasatkin, P. Kurr, B. Kniep, A. Trunschke, R. Schlçgl, *Angew. Chem. Int. Ed*. **2007**, 46, 7324–7327. *Angew. Chem*. **2007,** 119, 7465 –7468.
9. M. P. Mikhailova, K. D. Moiseev, T. I. Voronina, T. S. Lagunova, Y. P. Yakovlev, *Semiconductors,* **2007**, 41, 161–166.
10. Y. R. Yuan, M. A. A. Pudensi, G. A. Vawter, J. L. Merz, *J. Appl. Phys.* **1985**, 58, 397-403.
11. C. Chen, C.-T. Cheng, J.-K. Yu, S.-C. Pu, Y.-M. Cheng, P.-T.Chou, Y.-H. Chou, H.-T. Chiu, *J. Phys. Chem. B* **2004**, 108, 10687-10691.
12. P. Chou, C.-Y. Chen, C.-T. Cheng, S.-C. Pu, K.-C. Wu, Y.-M. Cheng, C.-W.Lai, Y.-H. Chou, H.-T. Chiu, *ChemPhysChem* **2006**, 7, 222-228.
13. S. Kaniyankandy, S. Rawalekar, S. Verma, H. N. Ghosh*, J. Phys. Chem. C* **2011**, 115, 1428 –1435.
14. F. Liao, B. T. Lo, D. Sexton, J. Qu, C. Ma, R. C.-T. Chan, Q. Lu, R. Che, W.-M. Kwok, H. He, et al., *ChemCatChem* **2015**, *7*, 230–235.
15. C. Eley, T. Li, F. Liao, S. M. Fairclough, J. M. Smith, G. Smith, S. C. E. Tsang, *Angew. Chem. Int. Ed.* **2014**, *53*, 7838–7842.
16. a) A. K. Singh, D. Pandey, S. Yoon, S. Baik, N. Shin, *Appl. Phys. Lett.* **2007**, 91, 192904. b) B. Lanson, *Clays Clay Miner*. **1997**, 45, 132–146. c) M. Yashima, S. Sasaki, Y. Yamaguchi, M. Kakihana, M. Yoshimura, T. *Mori, Appl. Phys. Lett*. **1998**, 72, 182. d) J. X. Wang, H. Y. Chen, Y. Gao, D. F. Liu, L. Song, Z. X. Zhang, X. W. Zhao, X. Y. Dou, S. D. Luo, W. Y. Zhou, et al., *J. Cryst. Growth* **2005**, *284*, 73–79.
17. F.-J. Zhang, F.-Z. Xie, S.-F. Zhu, J. Liu, J. Zhang, S.-F. Mei, W. Zhao, *Chem. Eng. J*. **2013**, *228*, 435–441.
18. F. Fresno, R. Portela, S. Suárez, J. M. Coronado, *J. Mater. Chem. A* **2014**, *2*, 2863–2884.
19. D. E. Bloom, *Science,* **2011**, 333, 562-569.
20. R. D. Cortright, R. R. Davda, J. A. Dumesic, *Nature,* **2002**, 418, 964-967.
21. G. A. Olah, *Angew. Chem. Int. Ed*. **2005**, 44, 2636-2639.
22. J. Tollefson, *Nature*, **2011**, 473, 134-134.
23. G. Bolye, *Renewable Energy—Power for a Sustainable Future,* **1996**, Oxford University Press: Oxford.
24. S. Malato, P. Fernandez-Ibanez, M. I. Maldonado, J. Blanco and W. Gernjak, *Catal. Today*, **2009**, 147(1), 1–59.
25. W. Y. Teoh, J. A. Scott and R. Amal, *J. Phys. Chem. Lett*., **2012**, 3, 629–639.
26. M. D. Hernandez-Alonso, F. Fresno, S. Suarez and J. M. Coronado, *Energy Environ. Sci*., **2009**, 2, 1231–1257.
27. J. M. Coronado, F. Fresno, M. D. Hernandez-Alonso and R. Portela (Eds), *Design of Advanced Photocatalytic Materials for Enegy and Environmental Applications*, Springer, London, **2013**.
28. R. D. Cortright, R. R. Davda and J. A. Dumesic, *Nature*, **2002**, 418, 964-967.
29. X. Chen, S. Shen, L. Guo and S. S. Mao, *Chem. Rev*., **2010**, 110, 6503-6570.
30. A. Fujishima and K. Honda, *Nature*, **1972**, 238, 37-38.
31. S. S. Mao and X. Chen, *Int. J. Energy Res*., **2007,** 31, 619-636.
32. T. Jia, A. Kolpin, C. Ma, R. C.-T. Chan, W.-M. Kwok, S. C. E. Tsang, *Chem. Commun*. **2014**, *50*, 1185–1188.
33. A. Cao, Z. Liu, S. Chu, M. Wu, Z. Ye, Z. Cai, Y. Chang, S. Wang, Q. Gong and Y. Liu, *Adv. Mater*., **2010**, 22, 103-106.
34. X. Zong, J. Han, G. Ma, H. Yan, G. Wu, C. Li, *J. Phys. Chem. C* **2011**,115, 12202–12208.
35. H. Yan, J. Yang, G. Ma, G. Wu, X. Zong, Z. Lei, J. Shi and C. Li, *J. Catal.,* **2009**, 266, 165–168.
36. L. Amirav and A. P. Alivisatos, *J. Phys. Chem. Lett*., **2010**, 1, 1051–1054.
37. B. O'Regan, M. Gratzel, *Nature*, **1991**, 353, 737-740.
38. K. Honda, A. Fujishima, *Nature*, **1972**, 238, 37-39.
39. H. Gerischer, *Electrochim. Acta* **1990**, 35, 1677-1699.
40. S. Licht, G. Hodes, R. Tenne, J. Manassen, *Nature*, **1987**, 326, 863-864
41. A. Descoeudres, Z. C. Holman, L. Barraud, S. Morel, S. De Wolf, C. Ballif, *IEEE J. Photovoltaics* **2013**, *3*, 83–89.
42. A. Morales-acevedo, *Solar Energy*, **2007**, *80*, 675–681.
43. K. Ernst, R. Engelhardt, K. Ellmer, C. Kelch, H. J. Muffler, MCh Lux-Steiner, R. Könenkamp *Thin Solid Films* **2001**, 387, 26-28
44. Q. Zhang, G. Cao, *Nano Today* **2011**, 6, 91-109

45. G. Zhang, S. Jiang, Y. Lin, W. Ren, H. Cai, Y. Wu, Q. Zhang, N. Pan, Y. Luo, X. Wang, *J. Mater. Chem. A* **2014**, 2, 5675–5681.
46. G. Wang, X. Yang, F. Qian, J. Z. Zhang, Y. Li, *Nano Lett.* **2010**, *10*, 1088–1092.
47. a) M. M. Lee, J. Teuscher, T. Miyasaka, T. N. Murakami, H. J. Snaith, *Science* **2012**, 338, 643–7. b) W. S. Yang, J. H. Noh, N. J. Jeon, Y. C. Kim, S. Ryu, J. Seo, S. Il Seok, *Science* **2015**, 10.1126/ science.aaa9272.
48. M. palaniappan, P. Gleick, L. Allen, M. Cohen, J. Christian-smith, C. Smith, *Clearing the Waters-A focus on water quality*., Pacific institute, **2010**.

49. A. Sorokin, B. Meunier, *J. Chem. Soc., Chem. Commun.* **1994**, 15, 1799.
50. A. Sorokin, S. D. Suzzoni-Dezard, D. Poullain, J. P. Noel, B. Meunier, *J. Am. Chem. Soc.* **1996**, 118, 7410-7411.
51. S. S. Gupta, M. Stadler, C. A. Noser, A. Ghosh, B. Steinhoff, D. Lenoir, C. P. Horwitz, K.-W. Schramm, T. J. Collins, *Science* **2002**, 296, 326-328.
52. T. Collins, *J. Acc. Chem. Res.* **2002**, 35, 782-790.
53. Y. Du, Q.S. Fu, Y. Li, Y. Su, *J. Hazard. Mater.* **2011**, 186, 491–496.
54. Y. Cheng, H. Sun, W. Jin, N. Xu, *Chem. Eng. J.* **2007**, 128, 127–133.
55. J. A. Byrne, P. Dunlop, J. Hamilton, P. Fernandezp-Ibanez, I. Polo-Lopez, P. Sharma, A. Vennard, *Molecules*, **2015**, 20, 5574–5615.
56. J. Choi, H. Park, M.R. Hoffmann, *J. Phys. Chem. C* **2010**, 114, 783–792.
57. T.Y. Ke, C.Y. Lee, H.T. Chiu, *Appl. Catal. A: Gen.* **2010**, 381, 109–113.
58. R. Leary, A. Westwood, *Carbon* **2011**, 49, 741–744.
59. B.K. Vijayan, N.M. Dimitrijevic, J. Wu, K. A. Gray, *J. Phys. Chem. C* **2010**, 114, 21262–21269.
60. C. Lazau, P. Sfirloaga, C. Orha, C. Ratiu, I. Grozescu, *Mater. Lett.* **2011**, 65, 337–339.
61. P. Christopher, D.B. Ingram, S. Linic, *J. Phys. Chem. C* **2010**, 114, 9173–9177.
62. A. Fujishima, X. Zhang, D.A. Tryk, *Surf. Sci. Rep.* **2008**, 63, 515–582.
63. H. Xu, G. Li, G. Zhu, K. Zhu, S. Jin, *Cat. Comm.* **2015**, *62*, 52–56.
64. T. Cao, Y. Li, C. Wang, L. Wei, C. Shao, Y. Liu, *J. Sol-Gel Sci. Technol.* **2010**, *55*, 105–110.
65. C. Leng, J. Wei, Z. Liu, *J. Nano. Res.* **2013**,15, 1643-1653.
66. M. Curri, R. Comparelli, P. Cozzoli, G. Mascolo, A. Agostiano, *Mater. Sci. Eng. C* **2003**, 23, 285-289.
67. P. Banerjee, S. Chakrabarti, S. Maitra, B. K. Dutta, *Ultrason. Sonochem.* **2012**, 19, 85 – 93.
68. M. Hoffmann, S. Martin, W. Choi, *Chem. Rev.* **1995,** 95, 69 – 96.
69. N. Daneshvar, D. Salari, A. Khataee, *J. Photochem. Photobiol. A* **2004**, 162, 317 – 322.
70. S. Khayyat, M. Abaker, A. Umar, M. Alkattan, N. Alharbi, S. Baskoutas, *J. Nanosci. Nanotechnol.* **2012**, 12, 8453 – 8458.
71. L. Chen, Y. Tu, Y. Wang, R. Kan, C. Huang, *J. Photochem. Photobiol. A* **2008**, 199, 170 – 178.
72. F. Peng, H. Zhu, H.Wang, H. Yu, *Korean J. Chem. Eng.* **2008**, 24,1022 – 1026.
73. P. Li, Z.Wei, T.Wu, Q. Peng, Y. Li, *J. Am. Chem. Soc.* **2011,** 133, 5660 – 5663.
74. C. Yu, K. Yang, Y. Xie, Q. Fan, J. C. Yu, Q. Shu, C. Wang, *Nanoscale* **2013**, 5, 2142 – 2151.
75. Y. Haldorai, J.-J. Shim, *Compos. Interfaces* **2013**, 20, 365 – 377.
76. A. McLaren, T. Valdes-Solis, G. Li, S. C. Tsang, *J. Am. Chem. Soc.* **2009**, 131, 12540 – 12541.
77. D. Li, H. Haneda, *Chemosphere* **2003**, 51, 129 – 137.
78. M. T. Uddin, Y. Nicolas, C. Olivier, T. Toupance, L. Servant, M. M. Müller, H.-J. Kleebe, J. Ziegler, W. Jaegermann, *Inorg. Chem.* **2012**, *51*, 7764–73.
79. F. Liao, Z. Zeng, C. Eley, Q. Lu, X. Hong, S. C. E. Tsang, *Angew. Chem.* **2012**, 124, 5934 – 5938; *Angew. Chem. Int. Ed.* **2012**, 51, 5832 – 5836.
80. M. Lee, K. Yong, *Nanotechnology* **2012**, 23, 194014.
81. V. Consonni, G. Rey, J. Bonaim, N. Karst, B. Doisneau, H. Roussel, S. Renet, D. Bellet, *Appl. Phys. Lett.* **2011**, 98, 111906.
82. Y. Liao, W. Que, J. Zhang, P. Zhong, Y. Yuan, X. Qiu, F. Shen, *J. Nanosci. Nanotechnol.* **2013,** 13, 959 – 963.
83. B. C. Gates, *Chem. Rev.* **1995**, 95, 511 –522.
84. P. G. Jessop, *in Handbook of Homogeneous Hydrogenation*,Vol. 1 (Eds.: H. de Vries, K. Elsevier), Wiley-VCH, Weinheim, **2007**, pp. 489 – 511.
85. T. Sakakura, J.-C. Choi, H. Yasuda, *Chem. Rev.* **2007**, 107, 2365 –2387.
86. J. G. Wu, M. Saito, M. Takeuchi, T. Watanabe, *Appl. Catal. A* **2001**, 218, 235 – 240.
87. G. C. Chinchen, P. J. Denny, J. R. Jennings, M. S. Spencer, K. C. Waugh, *Appl. Catal*. **1988,** 36, 1 – 65.
88. M. Saito, *Catal. Surv. Jpn.* **1998,** 2, 175 – 184.

Entry for the Table of Contents (Please choose one layout)

Layout 1:

MICROREVIEW

Heterojunction of two semiconductor phases to prolong lifetime for spatial charge separation is a well-established concept in photo-physics and is widely explored in solar cell and photocatalytic devices. However, its applications in thermal catalysis are currently rather limited. This min-review scoops the applications of nano-hetero-junction in thermal-catalysis area as to compare to photocatalysis with particular focuses on pollutants removal, renewable energy production and chemicals synthesis.

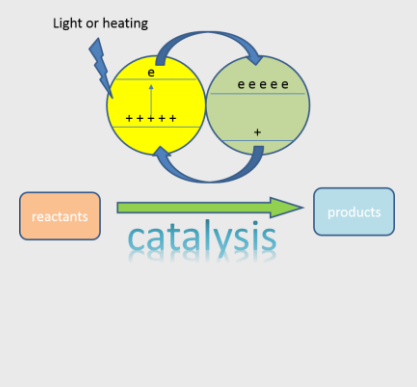

*Fenglin Liao, Benedict T.W. Lo, Shik Chi Edman Tsang **

Page No. – Page No.

The applications of nano-hetero-junction in optical and thermal catalysis